

TEST OF A MICROMEAS DETECTOR FOR THE MUON TRACKING CHAMBERS OF ALICE

J.P. Cussonneau, P.Lautridou, L.Luquin, V. Metivier, A. Rahmani,
V. Ramillien, T. Reposeur.

*Laboratoire SUBATECH, UMR Université - Ecoles des Mines - IN2P3/CNRS, F-44307
Nantes Cedex 03, France*

Abstract

An alternative solution for the muon tracking chambers of ALICE, based on the detector MICROMEAS [1], is investigated at SUBATECH. Three prototypes have been constructed and tested in the 3 GeV/c pion beam of the CERN PS. This paper describes the characteristics of these detectors, and the set-up used for the tracking test. Results concerning efficiencies and spatial resolutions as a function of gas mixtures, high voltages and the angular incidences of the particles are presented and discussed.

1 Principle of the chamber

This paragraph focuses on the characteristics of the prototype detectors built for the tests. A more general description of the working principle of the Micromegas can be found in the original paper of Y. Giomataris et al. [1]. Micromegas is a very asymmetric two-stage parallel-plate avalanche chamber working in proportional mode. The device is made of an anode strip plane, insulating spacers, a micromesh and a drift electrode. It operates in the following way: the primary electrons are produced in the 3 mm conversion gap

defined by the anode micromesh and the cathode foil. The amplification occurs in the $100\ \mu\text{m}$ gap between the microstrip plane and the micromesh. The avalanche field is obtained by applying a negative voltage in the range 400 - 700 V on the micromesh while a constant negative voltage of 1000 V is ensured on the conversion-drift electrode. The three detectors have been built strictly identical except one mesh which is slightly different from the two others for the square matrix (670 lines per inch instead of 500). Figure 1 exhibits a schematic view of one detector.

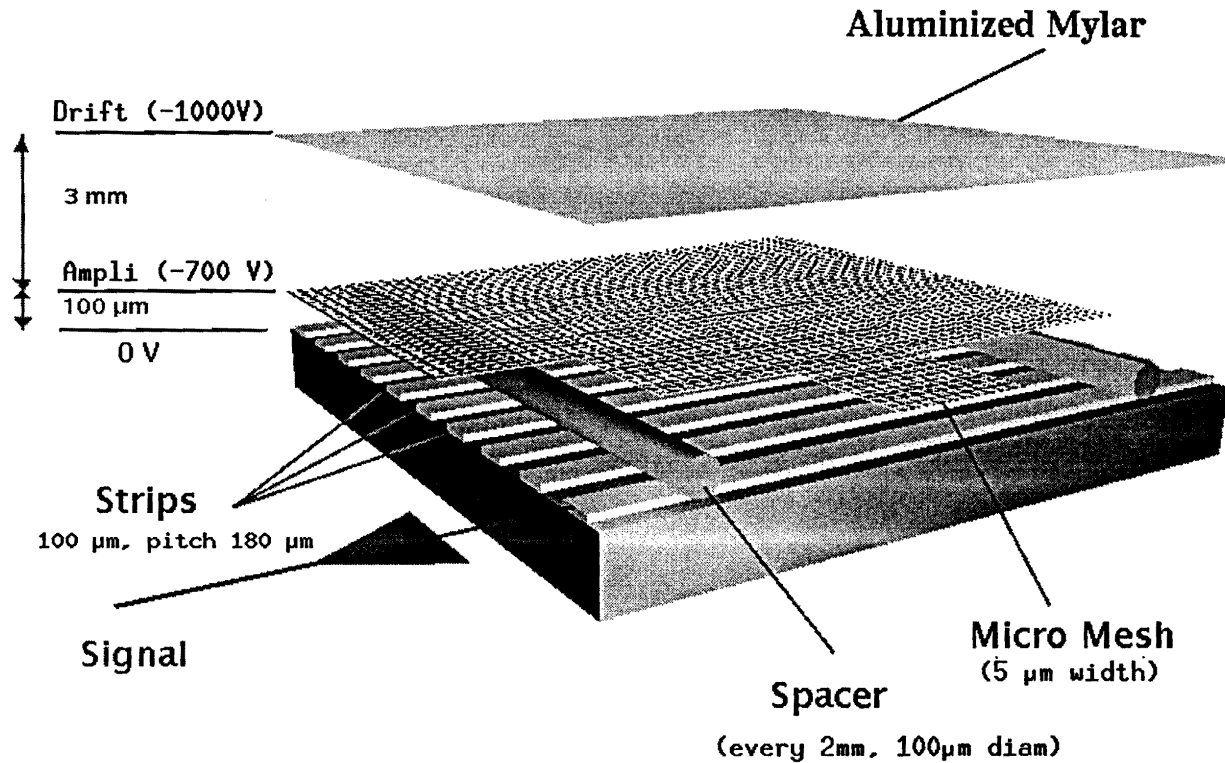


Figure 1: *Schematic view of one tracking plane of MICROMEAS used for the test. Scales between the four main structures are not relevant.*

Four functional structures can be isolated in the device:

- The anode electrode is made of an electronic board (GI 180) of 1.6 mm thickness on which are printed 336 parallel strips of $100\ \mu\text{m}$ width, $13\ \mu\text{m}$ thick ($10\ \mu\text{m}$ Cu covered by $3\ \mu\text{m}$ Au to prevent possible oxydation) with a pitch of $180\ \mu\text{m}$. These strips face directly the micromesh. Out of the active detector surface, one extremity of each strip is grounded to a charge preamplifier for the signal analysis. The total length of the strips including the blowing-out for the connectics reaches 35 cm. To avoid possible electromagnetic sources of perturbations, a standard ground plane ($35\ \mu\text{m}$ thickness of Cu) was deposited on the opposit side of the GI180 and on the overall board.

- The 100 μm amplification gap is defined by stretching spacer wires, every 2 mm on the GI 180 board, perpendicular to the main strip axis. Precise gap and good electrical insulation were obtained for these spacers by using a nylon fishing line of $100 \pm 2 \mu\text{m}$ diameter.
- The electroformed meshes are made of pure nickel square matrix $4.5 \pm 1.5 \mu\text{m}$ thick with a grid of 11.5 μm wide (11.5 μm) and 25 μm (39 μm) of hole for the 670 (500) lines per inch structures, respectively. The edges of the mesh are glued on a PVC rectangular frame of $6 \times 13 \text{ cm}^2$ inner opening which defines the active zone of the detector. With the high applied electric field, the mesh is layed on the insulating wires and the frame stays in position over the spacers by the mean of two small screws jointly liable for the GI 180.
- The 3 mm conversion drift gap is ensured by covering the opposite face of the 3 mm thickness mesh frame with a 6 μm aluminized mylar. This cathode plane is set to an higher voltage than the mesh to ensure the drift of the primary electrons.

The required gas tightness is obtained by surrounding the active area with another PVC box leaned against the GI 180 with a flange joint. A 100 μm mylar window covers the entrance of the detector. The gas mixture flushed at atmospheric pressure this box and the active area between the insulating wires. Under this configuration, a total radiation length $X_0 = 1.15 \%$ was reached per tracking plane. During the analysis stage, the corresponding scattering effect was taken into account.

2 Experimental set-up

For the test, a 3 GeV/c pion beam produced by the CERN PS accelerator was retained which corresponds almost to MIPS. We equally used π^- and π^+ particles with a contamination of about 30% of protons in this later case. The incident particles were tagged by the coincidence made with a pair of fast plastic scintillators NE102 ($5 \times 11 \text{ cm}^2$ and 6 mm thick) centered on the active area of the Micromegas detectors and set 30 cm upstream and downstream of the chambers. Estimation of the efficiency of the 3 Micromegas was deduced by counting the incident particles with a scaler in and out the acquisition dead time. Around 3000 incident particles illuminate the plastics each burst of 1 s. This coincidence triggered the Micromegas FEE based on 1008 Gassiplex [2] channels coupled to a V550 ADC of CAEN for the strips readout. Three CANBERRA 2003BT preamp. + ORTEC 570 ampl. connected to a LeCROY ADC 2249W analysed the 3 mesh signals. A complete acquisition chain built at SUBATECH and based on a LABVIEW + PC computer system was used to collect the experimental data from the CAMAC and VME crates. The three tracking planes, separated by 9 cm, crossed the particle path at the maximum of the beam profiles ($\sigma_H = 3 \text{ cm}$ and $\sigma_V = 1 \text{ cm}$). The main strip axis, positionned along the vertical direction of the middle detector, was allowed to rotate from 0 to 15° around this axis in order to investigate the spatial resolution versus the incident angle of the beam. A rough alignment between the strips of the 3 tracking planes was done at the assembling of the whole apparatus. About 420 μm of horizontal displacement was observed and corrected

at the analysis stage. Due to both the small divergence of the incident beam and the small active strip length (13 cm in vertical) of the chambers, the effects of the tilt angles between the 3 strips planes were estimated negligible and no correction was undertaken during the tracking procedure. The layouts of the set-up including the detectors is given in figure 2.

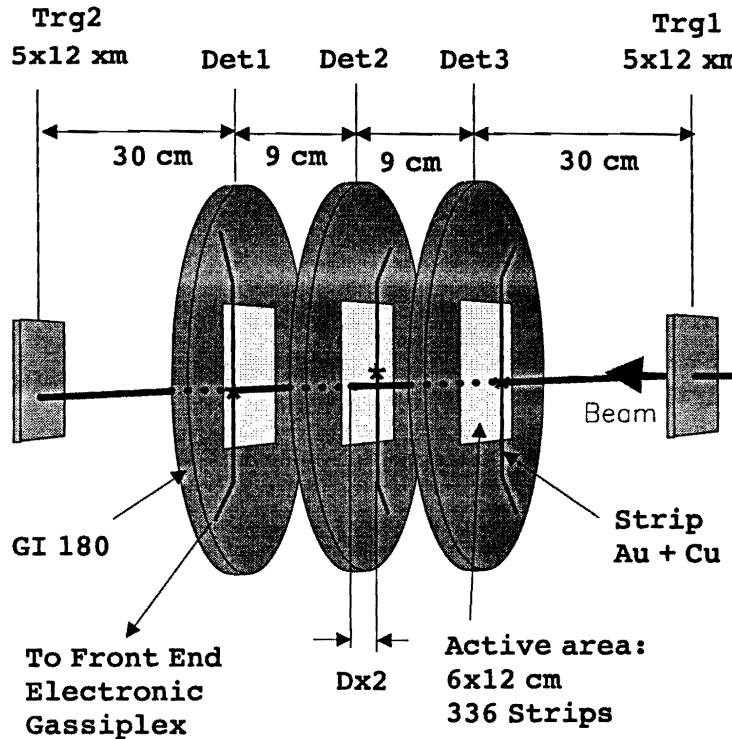


Figure 2: *Layout of the complete tracking set-up used for the beam test. The spatial resolution of the detector is derived from the tracking algorithm between the 3 planes only. A pivot centered on the vertical of the second tracking plane allows the whole set-up to rotate around the vertical axis.*

3 Experimental results

During the tuning phase of the detector, the energy resolution has been estimated using a sealed Fe^{55} radioactive source ($1 \mu\text{Ci}$) placed on the top of the drift electrodes. For indication, figure 3 shows the pulse-height distribution obtained when using the $\text{Ar}(74\%)/\text{CO}_2(26\%)$ mixture and the 590 V mesh voltage after analysis through the charge preamplifier and the spectroscopy amplifier with a $0.5 \mu\text{s}$ integration time. The 5.9 keV peak is clearly separated from the 3 keV Ar escape peak and the FWHM energy resolution reach 25 % with this uncollimated source. A gas gain of 10^4 was safely reached.

Before each data taking, pedestals and the thresholds of the ADC converter have been determined by triggering the readout of the gassiplex and V550 ADC chain at a random frequency. The associated distribution of charge of each strip was found gaussian shaped

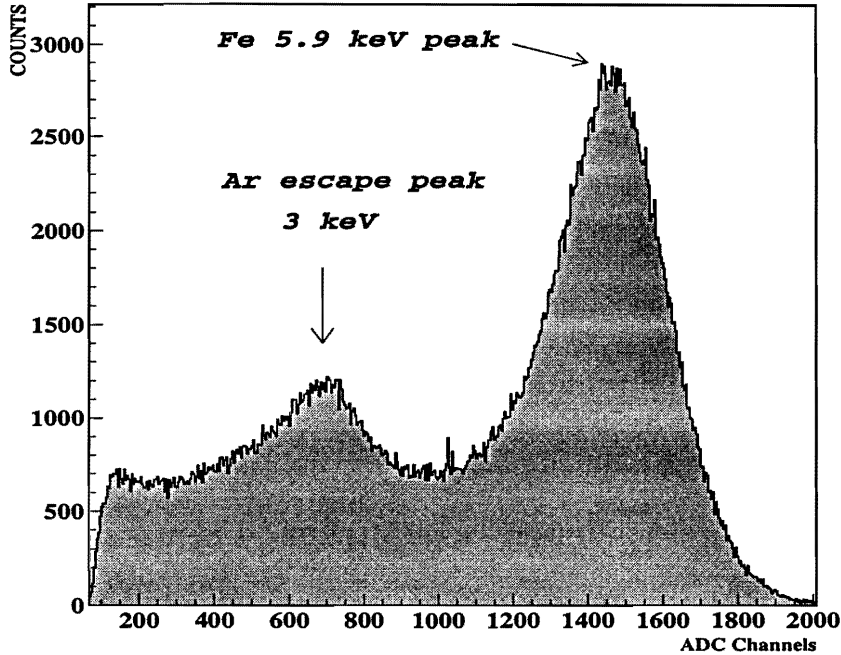


Figure 3: *Energy resolution of one detector with the Ar(74%)/CO₂(26%) mixture for the mesh voltage set to 590 V. The position of the 5.9 keV peak corresponds to a gain of 1.2×10^4 and an energy resolution of 25 % FWHM.*

with a maximum around 40 ch. and a RMS of 1.5 ch.. For each channel, the internal ADC threshold was set to the mean value plus 3 RMS when, for the pedestal subtraction, the internal ADC pedestal was set to the mean of the distribution.

The figure 4 shows the horizontal beam profile obtained when the detector was rotated by 7° around the vertical with respect to the beam direction. The strip patterns of planes 1 and 3 show the apparent displacement of the beam due to this rotation (the plane 2 is less affected because the vertical axis passes through it). Local inefficiencies observed for a few strips are mainly due to inappropriate ADC thresholds set at the converter level.

In order to evaluate the Micromegas performances in terms of spatial resolution and efficiency, one has to first determine the incident particle trajectories by the requirement of three aligned clusters in the tracking planes. A cluster is defined as the succession of contiguous fired strips with the possibility of one missing strip between two strip hits. The number of fired strips per cluster is shown in figure 5. On average, the cluster spatial extension covers 2 strips meaning that the lateral extension of the drift is less than 400 μm . This small value is due to the electric field configuration [1].

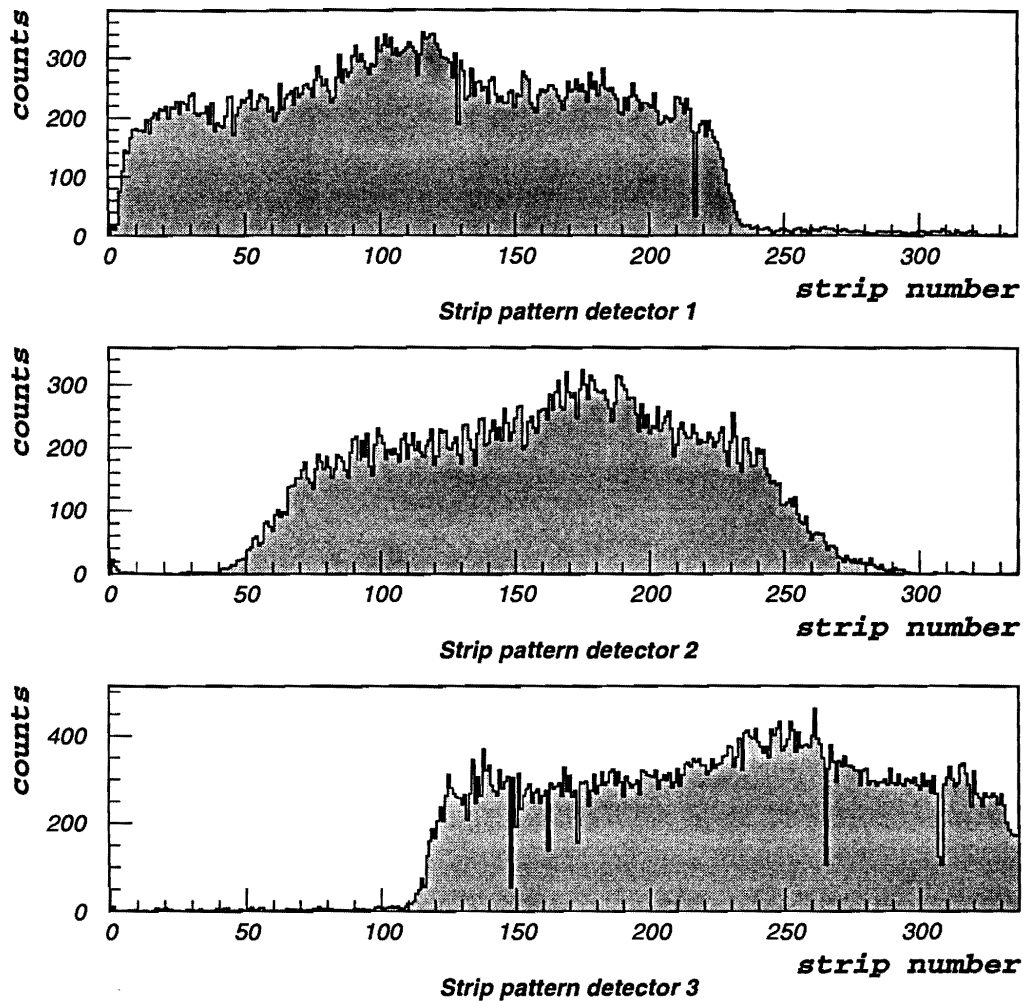


Figure 4: *Strip patterns of the 3 detectors obtained with an incidence angle of 7° during the run without subsequent filtering than converter thresholds and pedestals.*

Figure 6 shows the corresponding charge distribution of the clusters after recognition by the analysis program. Although no preamplifier calibration and correction have been done before the charge matching of the fired strips, a good behaviour of the charge distribution is observed.

Corresponding to an analogical or logical treatment of the signal, the cluster position is then calculated in two different ways (with the threshold cuts and the pedestal subtractions of the strip signals done at the converter level):

- as the center of gravity of the charge distribution in the *Analogical* case (this calculation was done without charge calibration for each strip)

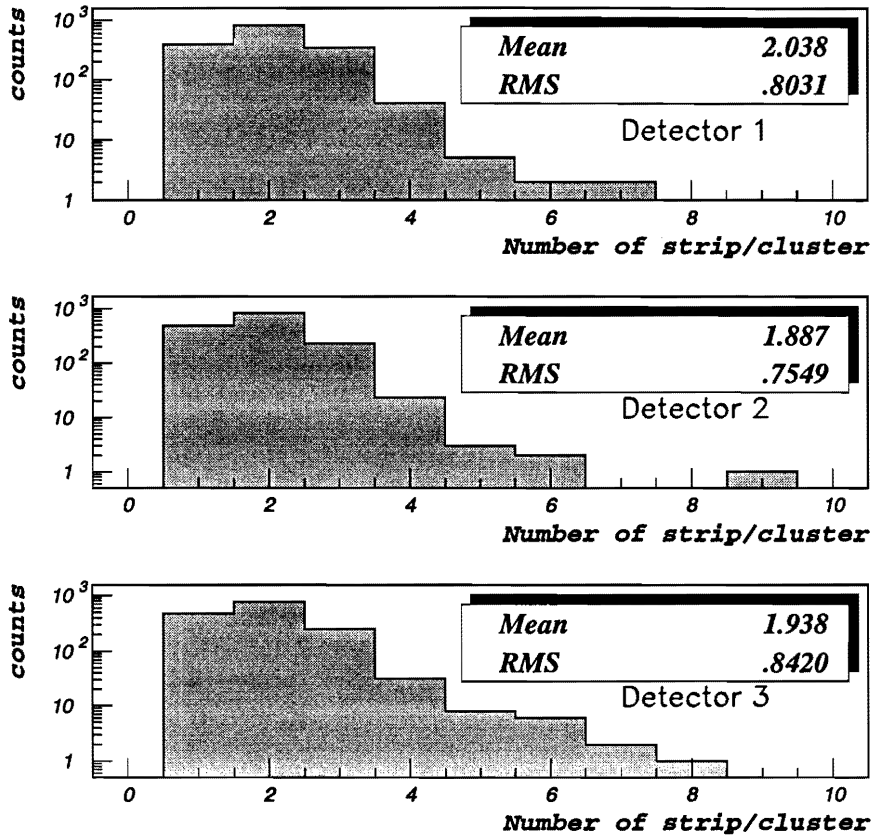


Figure 5: Distributions of the number of fired strips per cluster for the 3 detectors. The gas mixture was Ar(74%)/CO₂(26%) and $V_{\text{mesh}} = 590$ V.

- as the mean position of the fired strips in the *Logical* case

In order to estimate the spatial resolution of the detectors, the distance D_X between the cluster position in chamber 2 and the crossing point of the straight line extrapolation of the track defined by the two clusters in chambers 1 and 3 is computed for each incident particle (see figure 2). By the mean of this D_X distribution, one can directly deduce the spatial resolution from a gaussian fit of this D_X distribution in the *Analogical* case and from the RMS of this distribution in the *Logical* case.

It should be stressed that this method assumes that the spatial resolutions of the three detectors are the same; in other words we are not able to disentangle the resolution of each detector. Also, the results are corrected from the multiple scattering in the detector. Knowing that the Micromegas thickness is 1.15% radiation length, the resulting RMS dispersion on D_X is estimated to 21 μm . Figure 7 shows the distribution obtained with the two treatment modes.

Table 1 shows the spatial resolutions and the efficiencies as a function of the gas us-

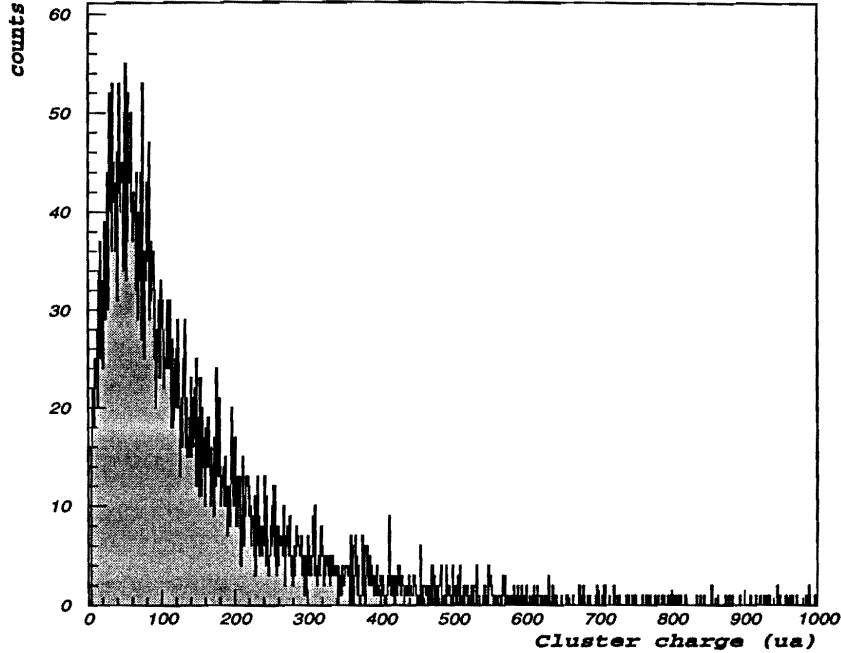


Figure 6: *Distribution of the total charge per cluster with the gas mixture Ar(94%)/CO₂(6%). The result is obtained without any charge calibration of the strips.*

ing Ar/CO₂ as well as Ar/Isobutane mixtures in both *Analogical* and *Logical* cases. For not too high ratio of quench gases (up to 30%), it is found that the resolution improves with this ratio. Indeed, table 1 seems to indicate that the cluster size (ie. the lateral development of the avalanche) decreases when increasing the quench gas ratio, inducing a more localized deposit charge of the particle. However, when the quench gas ratio gets too high, there is not enough fired strips to accurately calculate the clusters position and the resolution is getting worse reaching the waited classical value of $180/\sqrt{12} \simeq 52 \mu$. Concerning the counting rate performances, the efficiency was taken as the mean value from the total tracking efficiency of the three planes. Since the three detectors do not respond in the same way, the presented values must be considered as lower limits for the single-detector efficiency.

Table 2 shows the resolution as a function of the incidence angle for the Ar(74%)/CO₂(26%) gas mixture . A deterioration of the resolution for the large incidence angles (greater than 10°) is due both to the basic geometrical effect which increases the number of fired strips along the particle path in the drift gap and also to the nearly uniform distribution of charges on these fired strips. A small difference is observed between the analogical results and the logical results. This discrepancy could be imputed to the lake of charge calibration of the strip signals.

Table 3 shows the resolution and the efficiency as a function of the micromesh high

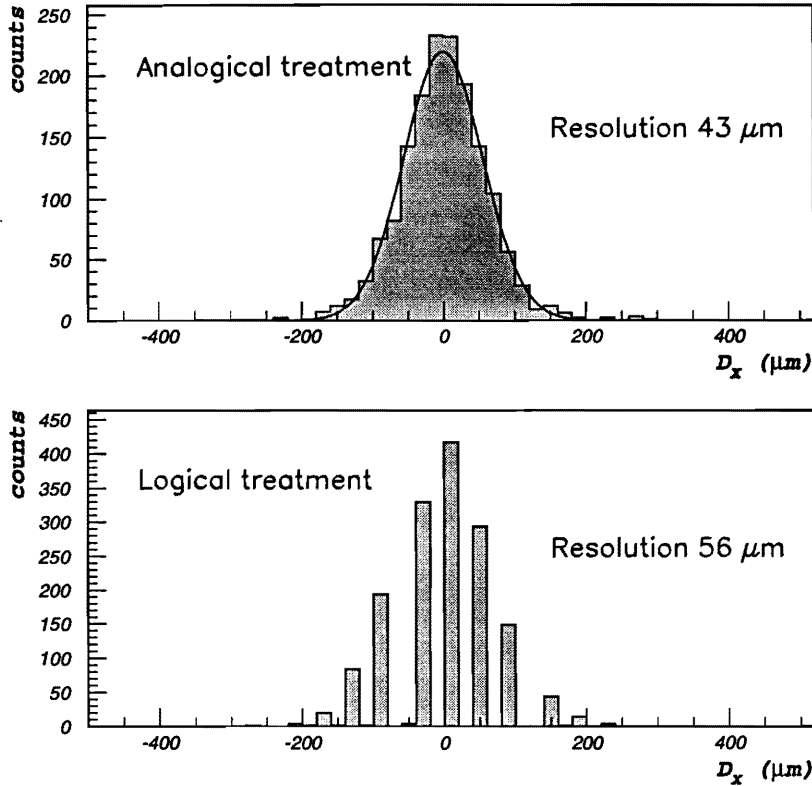


Figure 7: Distributions of the D_X parameter after analogical and logical analysis. The gaz mixture used was Ar(74%)/CO₂(26%) and the high voltages were set to 590 V and 1000 V for the mesh and the drift plane respectively.

voltage. The gas mixture is the one used to obtain the best resolution. It can be seen that the spatial resolution depends slightly on the high voltage. Nevertheless the efficiency increases with high voltage due to the gain improvement up to 94% for Ar(76%)/CO₂(24%) mixture. For higher voltage, sparks were generated in the amplification gap, inducing unstable runing conditions of the detector due to the mesh current limitation (100 nA) of the power supplies. In every cases of sparks, no damages were observed on the strips and the mesh planes as well as for the electronics.

4 Outlooks

In order to enlarge the possibilities of our Micromegas detectors to other working modes, several alternatives of treatment of the detector have been investigated with the data Ar(74%)/CO₂(26%) and $V_{\text{mesh}} = 590$ V.

One of the most simple possibility consists in reducing the present ADC resolution

	Ar/CO ₂				Ar/Isobutane		
CO ₂ or Isobutane in Ar (%)	6	14	26	47	12	20	43
efficiency (%)	92	93	94	94	88	89	82
Nb of strip per cluster	3.11	2.15	1.95	1.21	2.34	2.01	1.40
Analogical resolution (μm)	70	59	43	53	63	47	48
Logical resolution (μm)	85	73	56	58	75	62	56

Table 1: *Efficiencies and spatial resolutions obtained with different percentage of CO₂ and Isobutane in the Argon. Resolutions are given for analogical and logical cluster identification as described below. The mesh voltage was set to obtained the best resolution with a given gaz mixture.*

Incidence (°)	0	7.4	10.0	14.6
Projected drift(μm)	0	389	529	781
Analogical resolution(μm)	43	90	125	205
Logical resolution (μm)	56	88	117	193

Table 2: *Spatial resolutions obtained for several incidence angles with a gaz mixture of Ar(74%)/CO₂(26%). The projected drifts is the geometrical projection on the strip plane of the incident track. Resolutions are given for analogical and logical cluster identifications as described below.*

from 10 bits to a 6 bits linear converter. For this goal, the strip charge encoding has only been divided by the relevant conversion factor. We deduce a spatial resolution of 44 μm very close to the 43 μm of the analogical analysis. As expected, this result indicates that the ADC resolution used during the run was more than enough (taking account from the lack of calibration of the strip channels) and that low cost electronics could be used without spoiling the detector performances. With a 5 bits linear ADC, a value of 46 μm was derived when for a 3 bits linear ADC, a value of 54 μm was estimated.

An alternative solution to the logical one could be the use of a very fast front end-

	Ar(76%)/CO ₂ (24%)			Ar(80%)/Isobutane(20%)		
Mesh High Voltage (V)	540	560	590	530	560	580
efficiency (%)	68	67	94	50	71	89
Nb of strip per cluster	1.50	1.49	1.95	1.30	1.45	2.01
Analogical resolution(μm)	52	50	43	57	53	47
Logical resolution (μm)	60	64	56	62	61	62

Table 3: *Efficiencies and spatial resolution obtained with different mesh high voltages (the drift electrode are set to 1000 V). Resolutions are given for analogical and logical cluster identifications as described below.*

electronic with 3-threshold discriminators. This solution, which could be considered as a non linear 2-bit ADC analysis at first sight, leads to a better spatial resolution of the detectors. We have simulated this configuration using our strip ADC measurements with the three thresholds set to $S_1 = 0$, $S_2 = 20$ ch., $S_3 = 100$ ch. of the V550 ADC (the S_1 thresholds correspond to the ADC threshold-piedestal used during the run). We obtain a spatial resolution of $49 \mu\text{m}$ instead of $56 \mu\text{m}$ for the logical analysis and instead of $43 \mu\text{m}$ for the analogical analysis. These results indicate that the resolution still remains good enough even when using a faster and cheaper electronic.

In the same way, the resolution of our Micromegas detectors with an apparent double pitch of $360 \mu\text{m}$ has been tentatively evaluated with the present data. In this aim, we have associated successively two adjacent strips, and then used the same procedure to estimate the resolution. With the Ar(74%)/CO₂(26%) mixture, we obtain a spatial resolution of $78 \mu\text{m}$ ($83 \mu\text{m}$) for particles at normale incidence and $135 \mu\text{m}$ ($135 \mu\text{m}$) at 10° incidence in analogical and logical mode, respectively . These results seem to indicate that the performances of a $360 \mu\text{m}$ pitch detector remains acceptable for the requirements of the tracking chambers in the ALICE dimuon spectrometer.

5 Conclusion

For this first beam test, our experimental results indicate that most of the performances requiered for the ALICE dimuon tracking chambers [3] [4] are reached. Excellent spatial resolution is obtained both with an analogical and with a simulated logical treatment of the strip signals. This later result issues mainly from the small number of fired strips for 0° incident particles. As expected at larger angular incidences, the position barycenter tend to the charge barycenter of the fired strips. The resolution deduced from the logical analysis leads to the same quality than for the analogical mode and stays still in acceptable limits. Good efficiency is obtained using the very simple gas mixture Ar/CO₂, known to be quite inefficient to neutrons. No spark damage is observed even for very large gas gains at fields higher than 70 kVcm^{-1} . A full optimisation of the gas mixture is not achieved and improvements of the gas gains up to 10^6 is foreseen which opens the possibility to fit out Micromegas with extremely low cost electronics. Thanks to the fast electron + ion strip signal [5] (below 100 ns, rise time < 5 ns), fast current preamplifiers followed by discriminators and logical units could allow the Micromegas trackers to work as fast trigger chambers in the same setting. This promissing opportunity will be fully investigated next year. In the same hand, optimisation of the strips width and the maximum strips length will be carried on, using as more as possible conventional printing technologies on thin kapton subtrates, decreasing in the same time the total radiation length per tracking plane. Last but not least, juxtaposition of several mesh on the strip substrate has to be investigated in order to reach active surfaces of several m^2 . For the next year, our goal is to validate our building technic for modular avalanche-drift frames in a larger prototype of 1 m^2 by placing side by side several $24 \times 24 \text{ inch}^2$ meshes on a single piece strip-board.

Acknowledgements

We thank H. H. Gutbrod, director of SUBATECH, for his continuous support. We are very grateful to many colleagues for their continuous advice, especially G. Charpak, Y. Giomataris and his group of saclay. We are indebted to M. Labalme, M. Le Guay, P. Pichot for their unfailingly technical assistance for the mechanical and electronical realizations.

References

- [1] Y. Giomataris et al, Nucl. Instr. and Meth. A 376 (1996) 29-35.
- [2] W. Beusch et al., CERN/ECP/MIC Internal Note 4 (1993), and J. C. Santiard, CERN/ECP/MIC Internal Note 9 (1995)
- [3] ALICE Technical Proposal, The Forward Muon Spectrometer, CERN/LHCC/96-32.
- [4] J. P. Cussonneau et al., ALICE Internal Note 96-32.
- [5] F. Bartol et al., J. Phys. III France 6 (1996) 337-347

This report is also published in the ALICE collaboration under the reference
ALICE Note 97-28